JMEPEG (2009) 18:554–557
DOI: 10.1007/s11665-009-9457-z

1059-9495/$19.00

Analysis of Variant Orientation Before and After Compression in Polycrystalline $Ni_{50}Mn_{29}Ga_{21}$ MSMA

C. Hürrich, H. Wendrock, M. Pötschke, U. Gaitzsch, S. Roth, B. Rellinghaus, and L. Schultz

(Submitted October 6, 2008; in revised form April 14, 2009)

This paper deals with the microstructure and plastic deformation of $Ni_{50}Mn_{29}Ga_{21}$ ferromagnetic shape memory alloys. In contrast to conventional shape memory alloys, plastic deformation in the martensitic phase, which is due to twin boundary motion, may be caused not only by mechanical stress but also by an external magnetic field. The polycrystalline sample was prepared by directional solidification with a texture parallel to the heat flow. Afterwards, a heat treatment follows for chemical homogenization and stress relaxation in the austenitic state. The configuration of the twin boundaries was analyzed before and after compressing the samples. The microstructure after compression was related to the magnetic properties.

Keywords casting, electron microscopy, mechanical testing

1. Introduction

Ni-Mn-Ga magnetic shape memory alloys with a chemical composition close to stoichiometric composition Ni_2MnGa arouse big interest in the last few years. In the martensitic state, plastic deformation is related to twin boundary motion. The motion of twin boundaries in the martensitic phase due to a magnetic field was demonstrated for the first time in 1996 by Ullakko et al. (Ref 1). Most of the previous investigations in magnetic field induced strain (MFIS) have been performed with single crystals (Ref 2, 3) because of well-defined orientation relationship and low defect density. In order to find MFIS by twin boundary motion, the magnetically induced shear stress must be larger than the twinning stress (Ref 4). The magnetically induced stress is determined by the magnetic crystal anisotropy, the lattice strain and the crystallographic relations between the twin variants. The magnetically induced stress is given by $\sigma_{max} = m \cdot K_u \cdot s^{-1}$, where m is the Schmid factor, K_u is the magnetocrystalline anisotropy constant and the twin shear $s = 0.5 \cdot \left(\frac{a}{c} - \frac{c}{a}\right)$, where a and c are the martensitic lattice parameters (Ref 2, 5, 6). To increase the strain and reduce the stress for twin boundary motion in polycrystals, mechanical training is necessary. Because of this training effect less stress is necessary for twin boundary motion. The influence of mechanical training on the stress-strain relationship in martensitic polycrystalline $Ni_{50}Mn_{30}Ga_{20}$ has been shown by Gaitzsch et al. (Ref 7).

This article is an invited paper selected from presentations at Shape Memory and Superelastic Technologies 2008, held September 21-25, 2008, in Stresa, Italy, and has been expanded from the original presentation.

C. Hürrich, H. Wendrock, M. Pötschke, U. Gaitzsch, S. Roth, B. Rellinghaus, and **L. Schultz**, IFW Dresden, Institute for Metallic Materials, P.O. Box 270116, 01069 Dresden, Germany. Contact e-mail: c.huerrich@ifw-dresden.de.

The influence of the magnetic field to the stress-strain behavior was determined by Gaitzsch et al. (Ref 6). In comparison to our work, the following are examples of other work on polycrystalline NiMnGa samples. Ullakko et al. (Ref 8, 9) reported on MFIS in polycrystals and by thermo-mechanical treatment. But there is no information about the change in microstructure, the data are similar to the single crystal. Up to now no further papers with more details about MFIS in polycrystals were found. There are only some papers that describe a technological route of texture development in polycrystals (directional solidification and plastic deformation) (Ref 10, 11). In the present paper, we investigate the microstructure and the surface topography of polycrystalline $Ni_{50}Mn_{29}Ga_{21}$ samples were analyzed before and after compression. Also, the magnetic domain structure was determined after compression. The influence of stress on the twin boundary arrangement is investigated in order to find possibilities to improve the MFIS in polycrystalline $Ni_{50}Mn_{29}Ga_{21}$.

2. Experimental

The polycrystalline shape memory alloy $Ni_{50}Mn_{29}Ga_{21}$ was melted inductively and cast in a hot ceramic mold with a cold copper plate at the bottom of the cylindrical mold. With this method it is possible to achieve a coarse-grained and a textured microstructure by directional solidification (Ref 12). To achieve homogenization the samples were annealed for 48 h at 1000 °C under Ar/5% H_2 atmosphere. The texture was characterized by x-ray diffraction (XRD). Cubic samples with an edge length of 5 mm were cut erosively parallel to the direction of solidification which is preferably a [100] axis of the cubic high temperature phase (austenite). Afterwards, the samples were annealed for 14 h at 600 °C to relieve stress. This procedure had been shown to be effective by Gaitzsch et al. (Ref 13). The next step was grinding and polishing to achieve plane and parallel surfaces. To remove the working strain layer which forms due to grinding and polishing, an electrolytic etching with 25% (vol) HNO_3 in ethanol was used. The microstructure was analyzed by scanning electron microscopy (SEM), the

orientation of the grains by electron backscatter diffraction (EBSD), and the magnetic domains by magnetic force microscopy (MFM).

3. Results and Discussion

The structure of $Ni_{50}Mn_{29}Ga_{21}$ alloys is tetragonal in the martensitic state (5M) at room temperature and cubic in the austenitic state (Ref 14). The Curie temperature is approximately 100 °C.

The surface topography of the cubic sample shows regions of parallel lamellae which overlap each other mainly at the interface between two neighboring regions. A typical area of the cube surface having different kinds of lamellae was chosen to investigate the orientation via EBSD and the topography with the SEM. Figure 1 shows the SEM and EBSD pictures of the same area. The fine lamellar structures have boundaries between the lamellae.

They are parallel arranged in certain regions. Each set of parallel lamellae arose from a single austenite grain. The boundaries between these lamellae are twin boundaries and their overlapping is observable in the SEM picture. The EBSD map (Fig. 1b) shows the lamellae which are colored according to their orientation. It can be seen that there are only three martensitic variants marked with black (34%), grey (18%), and light grey (8%) with an index rate of 60% and a step size of 0.3 μm. The [001] direction of the unit cell is parallel to the *x*-axis (marked with black), parallel to the *y*-axis (marked with grey), and parallel to *z*-axis marked with light grey. Here, the directions are indexed in the tetragonal structure of the martensite (*I*4*mmm*). Thus, the [110] direction based on the tetragonal structure is parallel to the [100] direction in the cubic high-temperature phase.

A shadowing effect occurs due to the surface roughness and a tilt angle of 70°. Therefore, there are regions which could not indexed by the EBSD system. These regions are marked white in Fig. 1(b). Figure 1(c) shows the change in the orientation of the *c*-axis between the lamellae. The period between two lamellae is approximately 1.5 μm. The line scan was taken along the black line in Fig. 1(b).

A cubic sample was compressed successively along the solidification direction. The maximum stress was 40 MPa and after unloading the remanent strain is about 2% (Fig. 2).

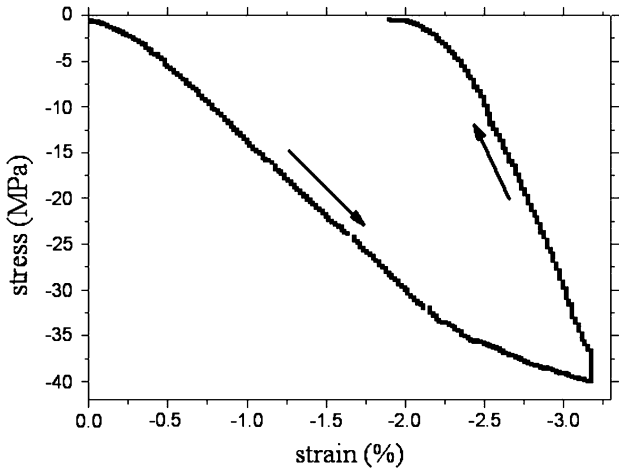

Fig. 2 Stress-strain curve of a 5M $Ni_{50}Mn_{29}Ga_{21}$ sample in solidification direction

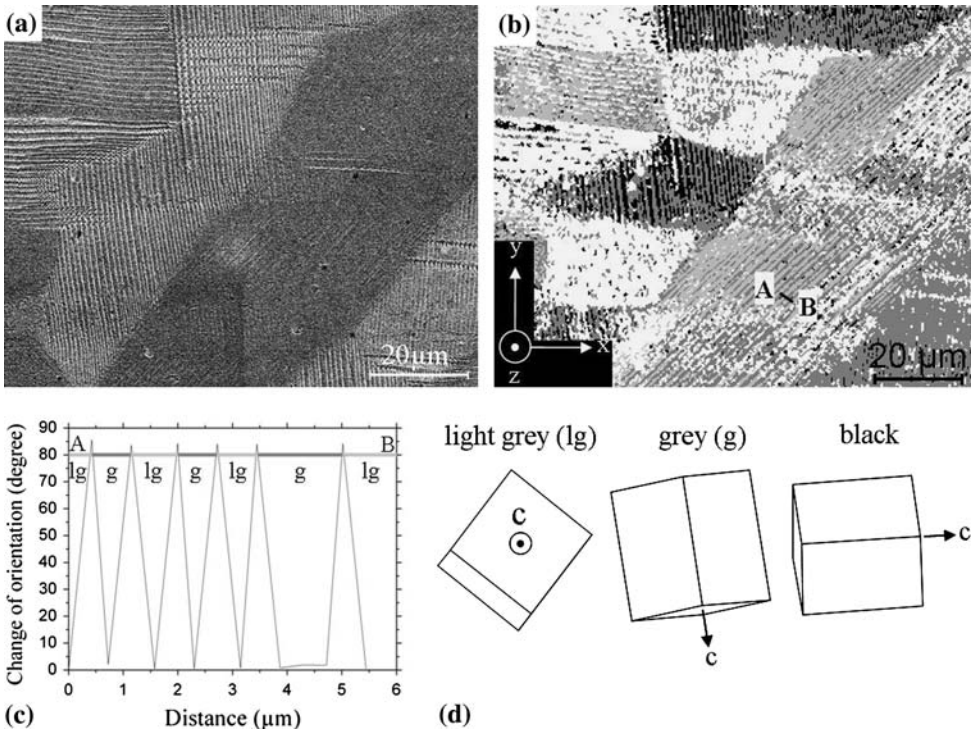

Fig. 1 Comparison of the topography by SEM (a) and orientation by EBSD (b, d) of the same area of NiMnGa with the change of orientation (c) along the black line in (b)

The twin boundaries are visible as height steps due to anisotropic etching. During the deformation process, twin boundary motion occurs, but the etched lamellae stay at the same place. Only a small tilting of the lamellae is observed because of the overall deformation of the sample. A very thin film develops on the surface which remains unchanged after etching the sample. After the deformation, a new preparation is not possible—to see the new microstructure—without changing the new twin structure. The reasons are compression force and shear force which affect the sample surface during polishing.

After compressing the sample, an EBSD picture taken from the same area is shown in Fig. 3 together with a line scan. The compressing direction is the same as the solidification direction. The twin distribution has changed dramatically. The grey colored areas where the *c*-axis is parallel to the compression direction increased and black colored regions, where the *c*-axis is perpendicular to it, are reduced. The index rate of Fig. 3 is 37%, with 31% grey, 5% black, and 1% light grey and the step size is 0.3 μm. There are only few black dyed regions. This means nearly the whole sample changed the orientation with the *c*-axis parallel to the compressing direction. A larger load would be necessary to remove the black dyed regions completely. The line scan shows that between all color changes the orientation of the *c*-axis changes by approximately 86°. This angle represents the orientation difference of the *c*-axis between the twins and can be calculated. From geometrical consideration it follows that the change in the orientation ϕ is given by $\phi = 2 \cdot \arctan\left(\frac{c}{a}\right)$ where the $\frac{c}{a}$ ratio is 0.94 for the 5M structure. A similar result was found by Cong et al. (Ref 15) for $Ni_{53}Mn_{25}Ga_{22}$ that each austenitic grain transforms to only two martensitic variants. After compression, the width of the martensitic variants with the *c*-axis parallel to the compression direction increased to about 7 to 11 μm.

Atomic force microscopy (AFM) and MFM images from the same area after compressing are shown in Fig. 4. The AFM (topography contrast) and MFM (phase contrast) are two

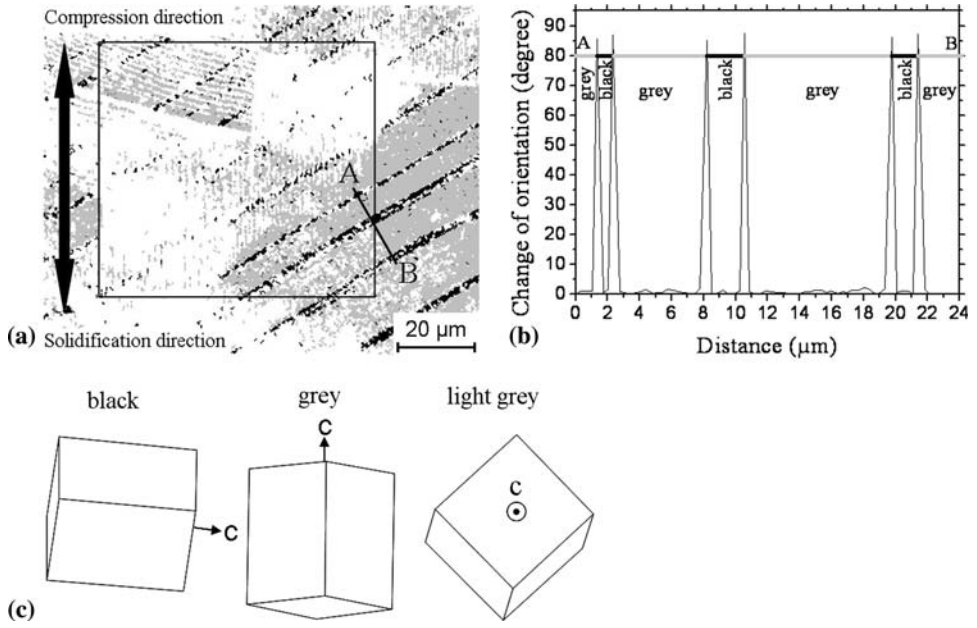

Fig. 3 (a) Orientation by EBSD after compression in solidification direction with (b) a line scan (black line in SEM picture) and (c) the direction of *c*-axes. The square marks the area which is shown in Fig. 4

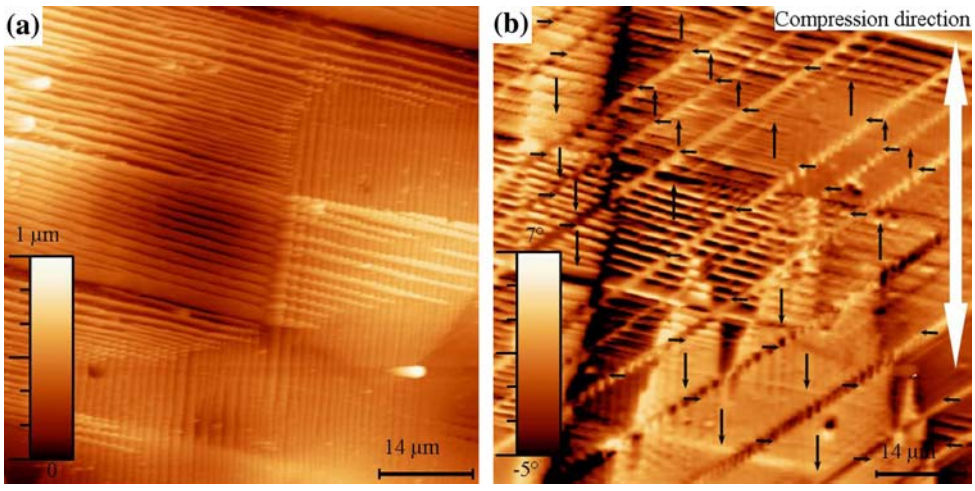

Fig. 4 (a) AFM picture (topography contrast) and (b) MFM picture (phase contrast) after compression of the same area like the EBSD image

different signals which were measured in the same scan. However, the AFM image taken after compression shows clearly those twins which were made visible by etching before compression and their overlapping while the MFM image reflects the twin distribution due to the magnetic anisotropy of the martensite after compression. The surface profile originated by etching shows the twin structure after compression and the height is 100 to 200 nm. This topography is also visible in the MFM picture but it is different from the domain contrast. The easy axis of magnetization is parallel to the *c*-axis. The EBSD image in Fig. 3(a) shows big areas with *c*-axis in *y* direction (grey), which is the compression direction. The square in Fig. 3(a) is the same area in Fig. 4(b). This area shows three big domains which are separated by 180° domain walls. The stripes corresponding to the black colored regions in Fig. 3 have another magnetic pattern. This contrast would be more intensive if there were 180° domains. The *c*-axis of the stripes is perpendicular to the compression direction. Two big domains are lighter than the background because the magnetization shows in the opposite direction which is also parallel to the compression direction. Also, the *c*-axis of the stripes can show in the opposite direction (arrows Fig. 4). Hence, no head-to-head configuration can be seen because of the stray field.

Comparing the MFM and the EBSD pictures, one can see that only with orientation sensitive methods the change of variant distribution by compression can be seen. SEM images are not suited for following the structure changes by, e.g., compression, because only the initial twin distribution is visible after compression due to topographic contrast produced by preparation. Both methods EBSD and domain observation by MFM show similar results.

4. Conclusion

The polycrystalline $Ni_{50}Mn_{29}Ga_{21}$ sample was prepared by directional solidification. The topography with its twin boundaries and the orientation of the twins fits very well before compression. After compression, the amount of those regions increases which have the *c*-axis parallel to the compression direction which is also the solidification direction in our case. It is possible to change the orientation of the *c*-axis in polycrystalline samples by compression. However, the surface topography did not change noticeable. Thus, observing the surface topography by optical microscopy or SEM is not suited for observing twin boundary motion during compression with this etch process. It is necessary to use orientation sensitive methods as EBSD or magnetic domain observation to follow the structural changes during compression.

Acknowledgments

The authors are grateful to A. Pöhl for technical assistance. The work was supported by DFG SPP 1239 code Ro 962/5.

References

1. K. Ullakko, J.K. Huang, C. Kantner, R.C. O'Handley, and V.V. Kokorin, Large Magnetic-Field-Induced Strains in Ni_2MnGa Single Crystals, *Appl. Phys. Lett.*, 1996, **69**(13), p 1966–1968
2. P. Müllner, V.A. Chernenko, M. Wollgarten, and G. Kostorz, Large Cyclic Deformation of a Ni-Mn-Ga Shape Memory Alloy Induced by Magnetic Fields, *J. Appl. Phys.*, 2002, **92**(11), p 6708–6713
3. R.C. O'Handley, S.J. Murray, M. Marioni, H. Nembach, and S.M. Allen, Phenomenology of Giant Magnetic-Field-Induced Strain in Ferromagnetic Shape-Memory Materials (Invited), *J. Appl. Phys.*, 2000, **87**(9), p 4712–4717
4. P. Müllner, V.A. Chernenko, and G. Kostorz, A Microscopic Approach to the Magnetic-Field-Induced Deformation of Martensite (Magneto-plasticity), *J. Magn. Magn. Mater.*, 2003, **267**, p 325–334
5. A. Sozinov, A.A. Likhachev, N. Lanska, and K. Ullakko, Giant Magnetic-Field-Induced Strain in NiMnGa Seven-Layered Martensitic Phase, *Appl. Phys. Lett.*, 2002, **80**(10), p 1746–1748
6. U. Gaitzsch, M. Pötschke, S. Roth, B. Rellinghaus, and L. Schultz, A 1% Magnetostrain in Polycrystalline 5M Ni-Mn-Ga, *Acta Mater.*, 2009, **57**, p 365–370
7. U. Gaitzsch, M. Pötschke, S. Roth, B. Rellinghaus, and L. Schultz, Mechanical Training of Polycrystalline 7 M $Ni_{50}Mn_{30}Ga_{20}$ Magnetic Shape Memory Alloy, *Scr. Mater.*, 2007, **57**, p 493–495
8. K. Ullakko, A. Sozinov, and P. Yakovenko, Large Magnetic-Field-Induced Strains in Ni-Mn-Ga Alloys due to Redistribution of Martensite Variants, Arxiv preprint cond-mat/0004211, 2000
9. K. Ullakko, Y. Ezer, A. Sozinov, G. Kimmel, P. Yakovenko, and V.K. Lindroos, Magnetic-Field-Induced Strains in Polycrystalline Ni-Mn-Ga at Room Temperature, *Scr. Mater.*, 2001, **44**, p 475–480
10. M. Pasquale, C.P. Sasso, S. Besseghini, F. Passaretti, E. Villa, and V.A. Chernenko, Effect of Texturing on the Magnetically Activated Properties of Polycrystalline NiMnGa Alloys, *J. Phys. IV France*, 2001, **11**, p 305–310
11. S. Besseghini, E. Villa, F. Passaretti, M. Pini, and F. Bonfanti, Plastic Deformation of NiMnGa Polycrystals, *Mater. Sci. Eng. A*, 2004, **378**, p 415–418
12. M. Pötschke, U. Gaitzsch, S. Roth, B. Rellinghaus, and L. Schultz, Preparation of Melt Textured Ni-Mn-Ga, *J. Magn. Magn. Mater.*, 2007, **316**, p 383–385
13. U. Gaitzsch, M. Pötschke, S. Roth, N. Mattern, B. Rellinghaus, and L. Schultz, Structure Formation in Martensitic $Ni_{50}Mn_{30}Ga_{20}$ MSM Alloy, *J. Alloys Compd.*, 2007, **443**, p 99–104
14. S. Roth, U. Gaitzsch, M. Pötschke, and L. Schultz, Magneto-Mechanical Behaviour of Textured Polycrystals of NiMnGa Ferromagnetic Shape Memory Alloys, *Adv. Mater. Res.*, 2008, **52**, p 29–34
15. D.Y. Cong, Y.D. Zhang, Y.D. Wang, M. Humbert, X. Zhao, T. Watanabe, L. Zuo, and C. Esling, Experiment and Theoretical Prediction of Martensitic Transformation Crystallography in a Ni-Mn-Ga Ferromagnetic Shape Memory Alloy, *Acta Mater.*, 2007, **55**, p 4731–4740